



# Contrast-modulation Flicker: Dynamics and Spatial Resolution of the Light Adaptation Process

SHENG HE,\*‡ DONALD I. A. MACLEOD†

*Received 4 February 1996; in revised form 13 November 1996; in final form 11 June 1997*

**We report a perceptual phenomenon that originates from a nonlinear operation during the visual process, and we use these observations to study the functional organization of the responsible nonlinearity: the regulation of visual sensitivity to light. When the contrast of a high frequency grating was modulated while its spatial and temporal average luminance was kept constant, observers saw brightness changes or desaturation in the field. If the contrast was modulated periodically between zero and a peak value, observers saw vivid flicker (contrast-modulation flicker), and this flicker could be seen even when the grating was too fine to be visually resolved as a pattern. This uniform-field flicker can be nulled by a modulation of space-average luminance at the contrast-modulation frequency, with appropriate phase and modulation depth. Contrast-modulation flicker is still measurable with gratings at 100 cycles/deg. The dynamics of contrast-modulation flicker suggest that it results from an early sensitivity-controlling mechanism, acting very rapidly (within about 20 msec). Its dependence on stimulus spatial frequency implies a strictly local luminance nonlinearity, one that either resides within individual photoreceptors or operates on signals from individual receptors. © 1998 Elsevier Science Ltd. All rights reserved.**

Light adaptation   Sensitivity control   Nonlinearity   Dynamics   Cone aperture

## INTRODUCTION

At its very earliest stage—the initial photochemical event—visual processing is linear (at normal light levels), but at later stages, after the signal has left the photoreceptors, nonlinearity abounds. That the regulation of sensitivity to light is a particularly important visual nonlinearity has long been recognized, yet there has been surprisingly persistent uncertainty as to the nature and locus of the nonlinear process. The earliest modern proposals were the contemporaneous ones of Maxwell and Fechner (Fechner, 1860; Maxwell, 1860). Maxwell invoked the independent saturation or overloading of the different cone mechanisms as the basis of the desaturation of intense lights. Fechner proposed a logarithmic nonlinear transformation of luminance, but in contrast to Maxwell insisted that physiological processing was linear and that the nonlinear transformation occurred in the relation between the physical and mental realms, a position soon challenged by the observations of Dewar and MacKendrick (1873), who saw in the electroretinogram evidence that a compressive, roughly logarithmic

nonlinear transformation of luminance is made already within the retina.

Clearly, the regulation of sensitivity should occur as early as practicable, if possible within the photoreceptors, so that even the early stages of the system can be protected from overload. Yet the existence of sensitivity-regulating mechanisms within the photoreceptors has been much debated. Currently, in some instances, functionally significant nonlinearity in the response to luminance has been demonstrated at the photoreceptor stage (e.g. Baylor, Hodgkin & Lamb, 1974; Boynton & Whitten, 1970), but in other cases (e.g. mammalian rods) the issue has not been completely settled (see reviews by Green, 1986; MacLeod, 1978; Shapley & Enroth-Cugell, 1984; Walraven, Enroth-Cugell, Hood, MacLeod & Schnapf, 1990; Koutalos & Yau, 1996).

Psychophysical attacks on the problem rely on the fact that signals from nearby photoreceptors are generally combined at later stages of processing. Thus, if sensitivity to light is regulated independently at different points in the visual field (Burton, 1973; MacLeod & He, 1993; MacLeod, Williams & Makous, 1992), or in different classes of photoreceptor (Williams & MacLeod, 1979; Chaparro, Stromeyer, Chen & Kronauer, 1995), the nonlinear light-adaptation process in question must be at a stage early enough for it to be fed by single cone inputs. It perhaps could for instance, reside within the receptors, although there is also the possibility of crosstalk between

\*Department of Psychology, University of Minnesota, 75 East River Street, Minneapolis, MN 55455, U.S.A.

†Department of Psychology, University of California at San Diego, La Jolla, CA 92093, U.S.A.

‡To whom all correspondence should be addressed. [Fax: 001 612 626 2079; Email: sheng@tc.umn.edu].

different photoreceptors (Baylor, Fuortes & O'Bryan, 1971). However, the psychophysical approach is hampered by the difficulty of controlling the light distribution on the retina. Contrast and edge sharpness are limited by diffraction and ocular aberrations. Even placement is uncertain, because of continuous involuntary eye movements. These problems can be alleviated by using an extended interference fringe pattern, generated directly on the retina, to stimulate the adaptation process (Burton, 1973; MacLeod & He, 1993; MacLeod *et al.*, 1992; Chen, Makous & Williams, 1993). Because it bypasses diffraction and other optical degradation, such a fringe can be much too fine for the observing subject to resolve perceptually, yet still be present at high optical contrast on the retina (MacLeod *et al.*, 1992). Burton (1973), MacLeod *et al.* (1992), and Chen *et al.* (1993) have demonstrated local adaptation with interference fringe patterns in photopic vision, by showing that two such patterns, overlapping but slightly misaligned can generate within the visual system a Moiré-like pattern known as a difference-frequency grating, which still appears when the primary fringe patterns are themselves individually too fine to be resolved perceptually.

We have recently reported (MacLeod & He, 1993) the phenomenon of "contrast-modulation flicker", another manifestation of visual nonlinearity observed with interference fringe patterns in human cone (photopic) vision: when we rapidly modulate the contrast of such a fringe (keeping overall luminance constant), a sensation of uniform field flicker results, even when the fringe is too fine to be perceived as a grating.

When contrast is modulated while keeping the overall luminance constant, as much light is always being added to the previously dark regions of the fringe pattern as is being subtracted from the light regions. In any spatial integration of linear responses to light, these effects should cancel out. The flicker seen during such a contrast-modulation implies a nonlinear visual response to local light intensity. It is particularly remarkable that this flicker, like difference-frequency gratings, can be generated by patterns that are subjectively unresolvable. Evidently the nonlinear stage is able to resolve fine patterns that are then obliterated by spatial integration at later stages of processing. This is what might be expected if the nonlinear stage resides within the cone photoreceptors themselves.

In this paper, we investigate contrast-modulation flicker in more detail and use it as a tool to explore the spatial and temporal properties of the underlying light adaptation mechanism. The nonlinear process injects into the visual pathway at the nonlinear site a distinctive signal, that depends on the input delivered to the nonlinear site by the earlier stages of the visual process and can, therefore, be used to characterize the visual system's representation of the stimulus at that site. The visibility of this product of nonlinear distortion will also depend on the characteristics of the later stages of processing, that transmit the distortion product signal from the nonlinear site. In our contrast-modulation flicker

experiments, we varied the spatial frequency of the fringe pattern to assess the spatial resolution of the system up to the nonlinear site. Variation of the temporal parameters addresses the dynamics of both subsystems—the ones responsible for the input to the nonlinear site and for transmission from it—but also, we will argue, the dynamics of the nonlinear mechanism itself.

Our results on spatial resolution of the nonlinear mechanism closely parallel those of MacLeod *et al.* (1992): contrast-modulation flicker, like difference-frequency gratings, can be seen as long as the photoreceptors themselves are differentially stimulated by the light and dark bars of the fringe. The nonlinear mechanism must therefore either be in the cone photoreceptors themselves (without substantial relevant cross-talk), or else (if postreceptoral) it must be fed by single cones, at a stage of processing prior to the neural spatial integration that prevents the fringe pattern from being resolved. Our results on the time-dependence of contrast-modulation flicker show that the mechanism involved is not a static, moment-by-moment compression of the response to instantaneous intensity; they suggest instead a dynamic sensitivity adjusting process with a very rapid (around 20 msec) response.

## STIMULUS

We rapidly modulate the contrast of a fine grating between a high value and zero while keeping its overall space-averaged luminance constant; subjects observe vivid flicker at the same rate as the contrast modulation (contrast-modulation flicker), as depicted in Fig. 1. The intensity of the basic contrast-modulated fringe pattern is:

$$I(x, t) = I_m \{ 1 + C[(1 + \cos(2\pi f_t t))/2] \cos(2\pi f_x x) \} \quad (1)$$

where  $C$  is the peak contrast of the fringe pattern,  $f_t$  is the temporal modulation frequency in Hz,  $f_x$  is the spatial frequency of the fringe pattern and  $I_m$  is the space-average luminance. As noted above, contrast-modulation flicker can be seen (despite the constancy of the space-average luminance) even when the grating is too fine to be directly resolved. Under these conditions, and also at high spatial frequencies within the resolvable range, contrast-modulation flicker can be nulled or minimized by a spatially uniform compensating modulation of the physical luminance at the contrast modulation frequency, with appropriate amplitude and temporal phase (Fig. 2). The field then appears not only devoid of stripes, but steady. In most of our experiments, the luminance modulation required for this subjective null provides an equivalent-input measure of contrast-modulation flicker. With nulling modulation,  $I_m$  in the above equation becomes:

$$I_m = I_o [1 + A_n \cos(2\pi f_t t + \Psi)] / 2 \quad (2)$$

where  $I_m$  is still the space-average luminance,  $I_o$  is the time- and space-average luminance,  $A_n$  is the amplitude of the nulling modulation of space-average luminance, and  $\psi$  is the relative phase between luminance and

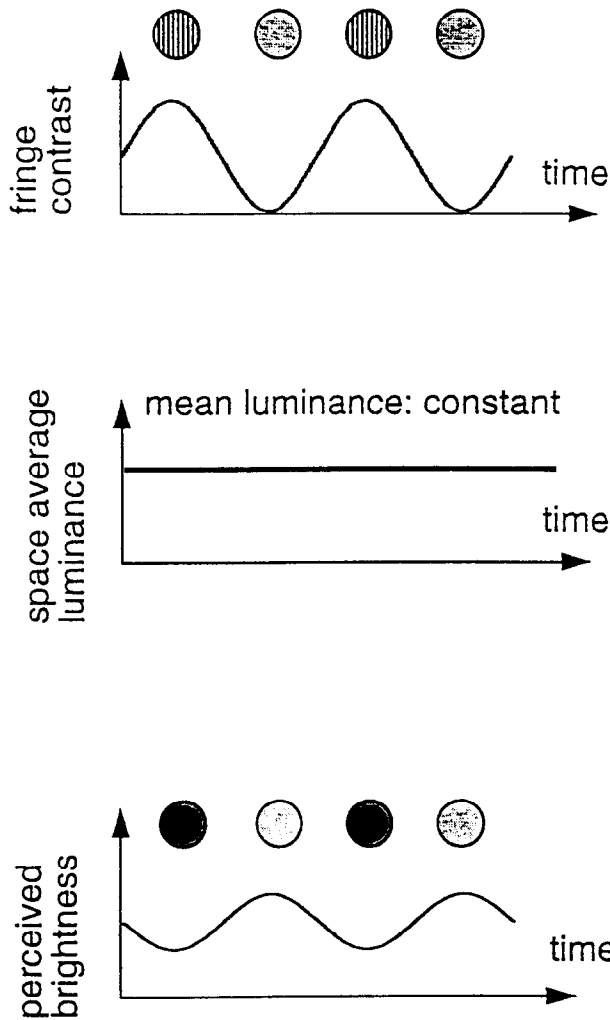


FIGURE 1. Stimulus and perception in contrast-modulation flicker. (A) Fringe pattern contrast varied sinusoidally between a peak value (generally unity) and zero. (B) Space average luminance was constant during the modulation of contrast. (C) Contrast-modulation flicker was seen.

contrast modulation. The fact that by adjusting  $A_n$  and  $\psi$ , a subjective flicker null can be achieved suggests that contrast-modulation flicker arises not simply from detection of any disturbance within the test field, but from a change in the effective overall brightness of the field when the grating changes its contrast\*.

The experiments reported in this paper were done on a laser interferometer described in detail elsewhere (He & MacLeod, 1996). The stimulus consisted of a small circular test field (50' in diameter) of coherent light

\*The nulls were generally well-defined (though we have no objective measure of this) but imperfect, especially at relatively low spatial and temporal frequencies. Perfect nulls are not theoretically expected. (For one thing, the theoretically appropriate luminance modulation to cancel a simple quadratic distortion product would be a rectified sine wave, so for the case of a simple quadratic nonlinearity the sine wave we used would cancel only the fundamental of the temporal modulation of effective luminance. But since the experiments quickly showed that the nonlinearity is not a simple one, we felt justified in adopting a simple sine waveform for the nulling modulation.)

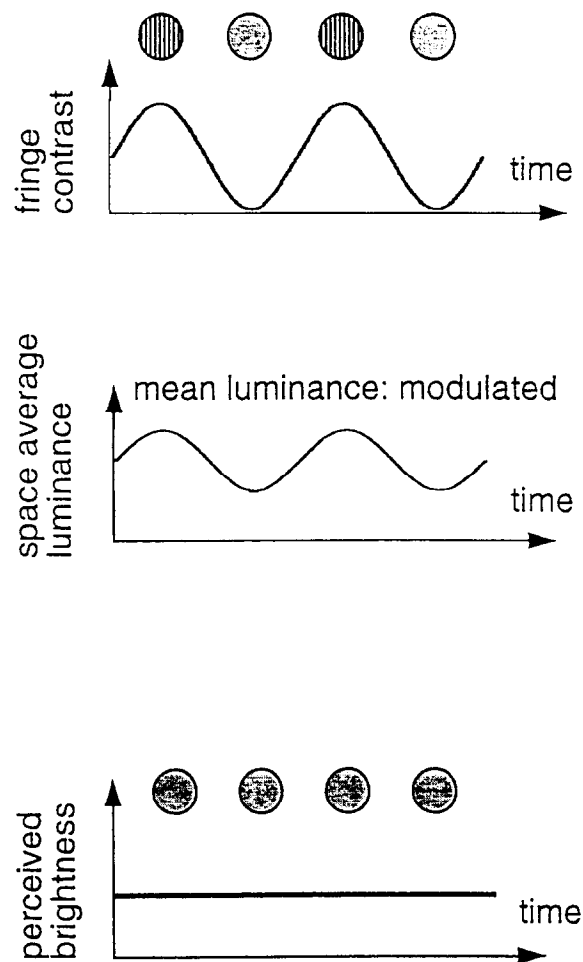


FIGURE 2. Nulling of contrast-modulation flicker. (A) Fringe pattern contrast varied sinusoidally as in Fig. 1. (B) Observer can adjust the phase and amplitude of space-average luminance modulation to minimize the perceived flicker. (C) Minimized perceived flicker, when the null was achieved.

embedded in a 10 deg surround of roughly equiluminant incoherent light. The test field was confined to the central fovea because only there are the cones small enough to preserve high optical contrast for fringes as fine as 100 cpd. The center test field was generated from a He-Ne laser (632.8 nm). The background was from incoherent light with its wavelength centered at 632 nm. Gratings with any desired spatial frequency could be generated in the center field from the interference of two light beams from the same laser source. Fringe patterns of high spatial frequency could be generated directly on the subject's retina with high contrast, and as shown in Fig. 1, their contrast could be modulated under computer control without detectable luminance change (less than 0.4% of luminance change when contrast is modulated between 0 and 1 at an average luminance level of 1000 td, see He & MacLeod, 1996).

Contrast-modulation flicker was measured in terms of the nulling luminance modulation at various spatial and temporal conditions. More detailed procedures and rationales are given in each of the experiments described below.

### EXPERIMENT 1: SPATIAL RESOLUTION OF THE NONLINEAR MECHANISM

Contrast-modulation flicker is expected if, at some stage where the grating is still resolved, each unit's response depends in a nonlinear way on light intensity, and the summed outputs from many such units determine the effective overall luminance of the field. If each unit's response is compressively nonlinear (or is adaptively regulated in sensitivity as discussed later), the space-averaged response will be greater for the uniform test field than it is for the grating. Figure 2 in MacLeod and He (MacLeod & He, 1993) conveys this idea. A mathematical description of how the space-average output from the nonlinear site will fluctuate with time can be found in Appendix I.

For contrast-modulation flicker to be seen, it is necessary that the fringe produce a sufficient spatial modulation at the input to the nonlinear mechanism. If prior optical blurring or linear neural spatial integration obliterates the fringe, the nonlinear mechanism will completely fail to "see" the contrast-modulated stimulus. The maximum fringe spatial frequency for which contrast-modulation flicker is visible is therefore a measure of the resolution of the visual system at the nonlinear site. Our experiments characterize resolution quantitatively using a measure of contrast sensitivity at the nonlinear site for a range of spatial frequencies. The general rationale is similar to that of a previous study (MacLeod *et al.*, 1992) of difference-frequency interactions between pairs of fringes, and is described more fully in that paper.

Using a nulling procedure, we measured the equivalent amplitude [ $A_n$  in equation (2)] for various fringe pattern spatial frequencies. The neural spatial filtering after the nonlinear stage will be independent of the spatial frequency,  $f_x$ , of the contrast-modulated fringe pattern, since both the measured and measuring signal were spatially unstructured. The amplitude of the distortion product depends on the amplitudes of the linear signals—fringe pattern contrast—at the input to the nonlinear site. As shown in Appendix I, nulling amplitude is expected to be roughly inversely proportional to the square of the spatial contrast attenuation factor at the input to the nonlinear site. Measuring the equivalent amplitude of the contrast modulation flicker as a function of grating spatial frequency allowed us to estimate the effective contrast at the input to the nonlinear site, thus the spatial dimension of the responsible nonlinear units (see Appendix I), and associate the units with known anatomical landmarks in the visual pathway.

To check the assumed approximately quadratic relationship between contrast-modulation flicker amplitude and peak input contrast, we also measured nulling amplitude as a function of grating peak contrast.

#### Procedure

To investigate the spatial frequency dependence of the nulling amplitude  $A_n$  [equation (2)], the contrast was modulated from 0 to 100% at each spatial frequency. A

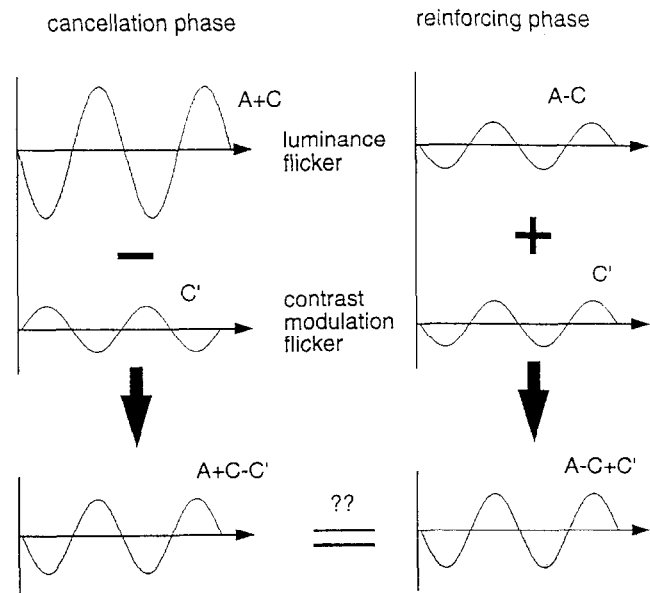


FIGURE 3. Pedestal-aided nulling procedure. In this arrangement, any failure to null the contrast-modulation flicker revealed itself as a difference in the resultant flicker amplitude between these two intervals. Contrast-modulation flicker could be measured more precisely with this method. See text for details.

contrast-modulation frequency of 15 Hz was found to give precise nulls, consistent with the high flicker sensitivity found at that frequency (Kelly, 1961). The phase of the nulling modulation [ $\psi$ , equation (2)] was chosen to place the luminance peak at 25 deg in advance of the contrast peak. This nulling phase was selected on the basis of a preliminary experiment in which the observer used a trackball to vary continuously and simultaneously both the amplitude (trackball  $x$ ), and the temporal phase (trackball  $y$ ), of a 15 Hz temporal modulation of whole field luminance in an effort to minimize or eliminate perceived flicker. Figure 2 shows the time course of the stimuli. Both observers found the best nulls when the nulling luminance peak slightly preceded the contrast peak (by between 0 and 50 deg). We therefore fixed the phase for the nulling signal at 25 deg in the main experiment, although measurements of the nulling amplitude  $A_n$  were quite similar without that phase advance; this is fortunate since despite subsequent investigation of this point (Experiment 2 below), we have no precise indication as to the optimal phase advance within this range under near-threshold conditions.

The straightforward nulling procedure of the preliminary experiment worked well when the contrast-modulation flicker was easily visible, but this method was less sensitive at the highest spatial frequencies of interest, when the contrast-modulation flicker was near or below threshold. In the main experiment we therefore adopted a refinement of the method which we term "pedestal-aided nulling" (Fig. 3), which exploits the fact that small differences in flicker amplitude around the just-detectable "threshold" amplitude,  $A$ , can be reliably detected even when the difference,  $\Delta A$  is much less than  $A$ .

(Henning, MacLeod and Stockman, unpublished). The subjects' task was to equate the visibility of the flicker seen during two different 1 sec intervals indicated by two tones. In the first interval, a physical luminance modulation was added to the contrast-modulation stimulus in cancellation phase. In the second interval, a slightly different luminance modulation was added in the opposite, reinforcing phase. The physical modulation of space-average luminance was selected to provide clearly visible flicker during both intervals. The subject could adjust the difference in modulation between the two intervals about a fixed average modulation. This is illustrated in Fig. 3, where the physical luminance modulation is  $A + C$  in the cancellation phase interval, and  $A - C$  in the reinforcing phase interval;  $C$  is adjusted by the subject. If  $C = 0$ , there is no difference in physical luminance modulation between the two intervals, but the addition of contrast-modulation flicker  $C'$  then makes the flicker more visible during the reinforcing interval. The subject can equate the flicker during the two intervals by adjusting the value of  $C$  using the trackball, and the value of  $C$  that achieves this subjective equality is the equivalent amplitude of the contrast-modulation flicker (Fig. 3). The equivalent amplitude can be determined with a precision of  $\Delta A/2$ , allowing measurements even when contrast-modulation flicker is not visible by itself.

Two observers participated in this experiment. The base luminance modulation amplitude  $A$  was set at a level according to some preliminary trials to provide a precise estimate of  $C'$ ;  $A$  was usually between 25 and 45%.

The experiment was repeated for a range of spatial frequencies in order to define the loss of effective contrast for high fringe frequencies at the input to the nonlinear mechanism. We also established the relationship between the depth of the contrast modulation and the resultant flicker amplitude, by modulating the contrast between zero and some chosen peak contrast rather than unity, and finding how much luminance modulation  $C$  is required to balance the flicker in the two intervals.

*Results and discussion*

Within a range of spatial frequencies (up to about 100 cpd), when fringe contrast was fully modulated without any nulling luminance modulation, observers experienced a clear sensation of flicker. When they increased the nulling signal with appropriate phase, the flicker decreased gradually to a point when it was hardly noticeable. If the observer kept increasing the amplitude of nulling signal past the null point, the flicker appeared again or increased in amplitude.

With the pedestal-aided nulling procedure used for the measurements presented here, the overall luminance modulation required (for unity peak fringe contrast) ranged up to about 40% (an excursion of about 2:1 between maximum and minimum luminance), depending on the spatial frequency of the grating. Values obtained without the pedestal were roughly consistent with these, but slightly smaller (by a factor of about 0.8) and more variable. The small effect of the pedestal on equivalent

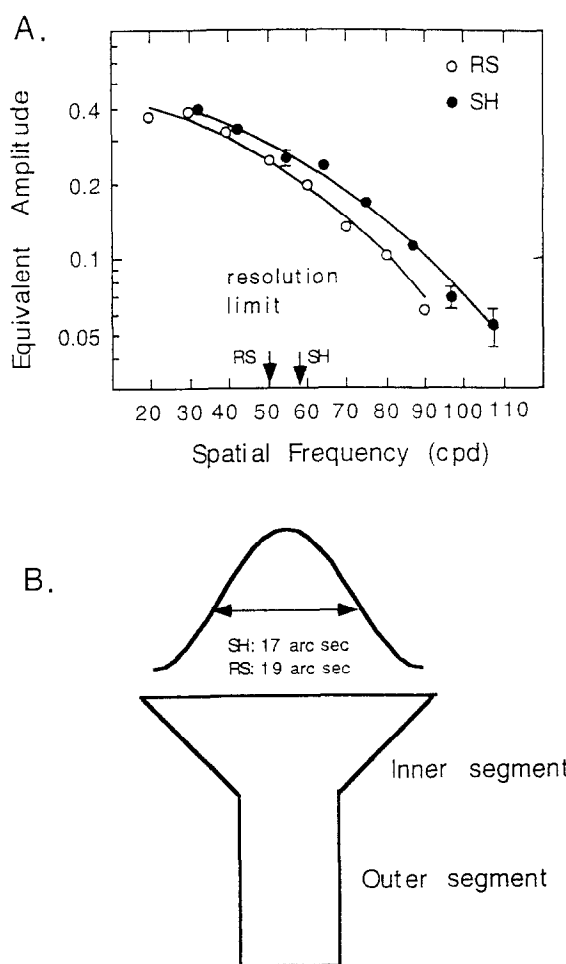


FIGURE 4. (A) Contrast-modulation flicker as a function of fringe spatial frequency for test fields fluctuating sinusoidally at 15 Hz between unity contrast and zero contrast. The equivalent (nulling) luminance modulation approaches 40% (a sinusoidal modulation of overall luminance between 1200 and 2800 trolands) at low fringe frequencies, and decreases only slowly with increasing frequency, remaining measurable at 100 cpd. Filled circles, SH; open circles, RS. Curve is the best-fitting gaussian. (B) Point spread function for light intensity at the input to the nonlinear element, compared with the dimensions of a central foveal cone. Effective contrast at the input to the nonlinear element was assumed proportional to the square root of the equivalent amplitude from (A); corresponding radially symmetrical point spread function is given by the Fourier transform of the function relating effective contrast to spatial frequency. Error bars in this and other figures represent  $\pm 1 \times$  the standard error of the mean (SEM), based on intersession variance (the variance of session means), divided by the number sessions, so that independence of errors within a session is not assumed. For RS, the number of sessions per point was not always enough to allow this.

amplitude is qualitatively predicted by the nonlinear models described in the Discussion section.

Figure 4(A) shows the contrast-modulation flicker amplitude measured through nulling at different grating spatial frequencies for two observers. The finer the grating, the less the flicker, but the equivalent amplitude decreases only very slowly as the fringe spatial frequency increases past the visual resolution limit (about 50 cpd for observer RS and about 57 cpd for observer SH, as shown by the arrowheads). Contrast-modulation flicker is still measurable even above 100 cpd. Evidently, the respon-

sible nonlinear elements resolve optical detail much better than does the entire visual system of the human observer. If the nonlinear response that produces contrast-modulation flicker is within the photoreceptor cells, then the grating only need be resolved with high contrast at the photoreceptor level, but not necessarily perceptually. The flicker amplitude should then depend entirely on the fringe contrast as seen by the cones themselves, which is limited mainly by the size of the individual cone receptors. This idea is supported by our results, and by the following analysis.

Figure 4(B) shows just how little spatial integration of light intensity at the input to the nonlinear elements is implied by the results of Fig. 4(A). The gaussian curve is the radially symmetrical point spread function corresponding to the frequency response curve of Fig. 4(A) (see also Appendix I for more detailed description of how the gaussian curve was derived). Evidently the nonlinearity is preceded by spatial integration of light intensity over a region spanning only 17.2 and 19.0 sec of arc for SH and RS, respectively (full width at half height). This is equal to the smallest histological estimate of the diameter of the light-collecting inner segment of the central foveal cones (Curcio, 1987; Polyak, 1941), and provides a functional estimate of the diameter of the cone's light-collecting area that is in rough agreement (see General Discussion) with the one from measurements of the visibility of another product resulting from local nonlinearity, the difference-frequency grating (Burton, 1973; Chen *et al.*, 1993; MacLeod *et al.*, 1992). The contrast of the primary gratings needed at different spatial frequencies to produce a threshold level difference-frequency grating of fixed spatial frequency—or, in our experiment, a criterion amplitude of contrast-modulation flicker—reflects only neural spatial filtering before the nonlinear site. In that sense, both experiments bypass neural resolution losses subsequent to the nonlinear mechanism, and allow an assessment of any neural resolution losses prior to that stage. The results of both experiments agree, in indicating that there are no neural resolution losses prior to the nonlinear mechanism. The nonlinear process is therefore local and early: either it is inside the cones themselves, or else it operates independently on the signals from each cone, before further spatial integration obliterates the representation of the finest fringes at later neural stages and perceptually.

Figure 5 shows that contrast-modulation flicker amplitude increases roughly as the square of the peak contrast: a reduction of peak contrast from unity to about 0.3 reduces the flicker amplitude roughly ten-fold from its unity-peak-contrast value of about 35%. This roughly quadratic growth with contrast is expected, if contrast-modulation flicker is generated by a smooth nonlinear transformation of luminance, since the modulation of space-average output increases roughly as a quadratic function of grating contrast for most compressive functions (see Appendix I). The fact that the contrast-modulation flicker was canceled by modulating the

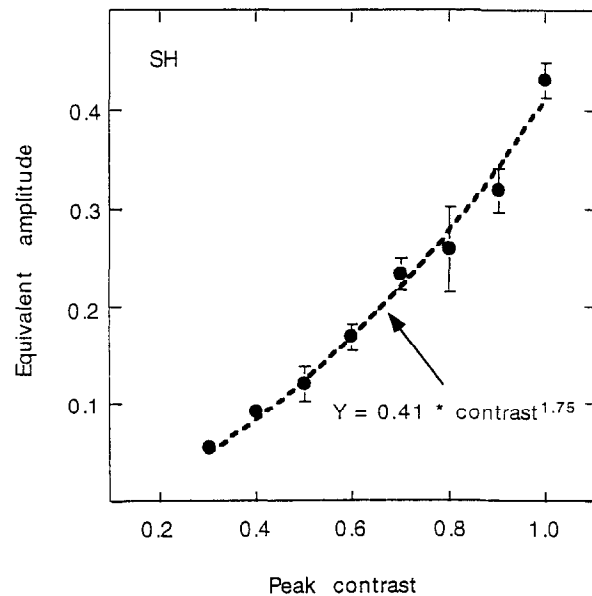


FIGURE 5. Contrast-modulation flicker as a function of peak contrast. Data are fitted with a power function with exponent as a free parameter. Contrast-modulation flicker is roughly a quadratic function of peak contrast.

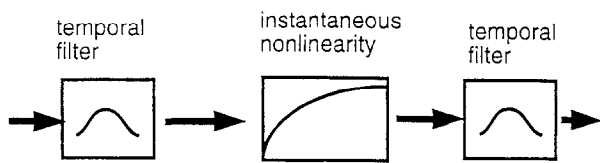
space-average luminance in approximate temporal synchrony with the contrast-modulation is indeed consistent with a compressive, not an expansive, nonlinearity, but the need for a slight phase advance of the nulling luminance modulation suggests that the nonlinearity is a time-dependent process rather than an instantaneous compression. This observation is taken further in the next experiment.

## EXPERIMENTS 2 AND 3: DYNAMICS OF LIGHT ADAPTATION

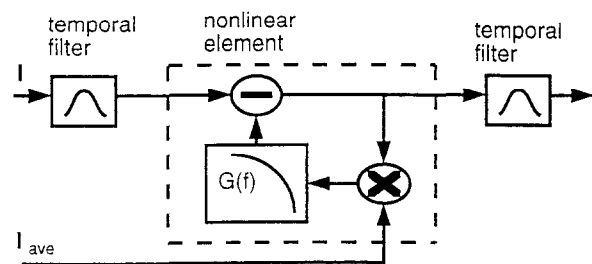
### *Experiment 2: factoring out earlier and later filters*

It is difficult to get at the dynamics of light adaptation psychophysically, for two reasons: (1) transient stimuli may produce sensitivity losses by overloading more central neurons, as well as by their action on the light-adaptation mechanism(s) of interest. (2) It is hard to allow for temporal filtering of the signals before and after the adapting element and isolate the intrinsic dynamics of the adaptation process itself. The technique of nulling contrast-modulation flicker provides a way around both these obstacles. First, the null is presumably determined at the output of the nonlinear element, and before spatial integration. This should help isolate the primary adaptation mechanism, because later stages of the system do not receive a time-varying signal: temporal filtering and masking at later stages are precluded (to the extent that the null is a good one). Temporal filtering on the way to the adaptation site will also not affect the null setting, for suitably chosen stimuli and system idealizations (Appendix I). For instance, in models where adaptation works by setting the parameters of a linear system in accordance with the time-average input intensity (Tran-

(a). Instantaneous Compressive Nonlinearity:



(b). Sluggish Nonlinear Feedback Model



(c). Sensitivity regulating model

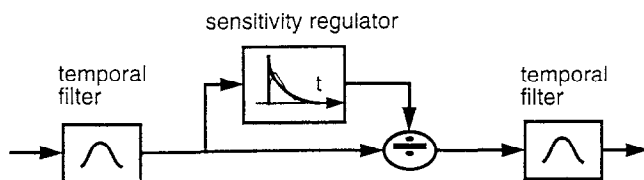


FIGURE 6. Three possible models. (A) Instantaneous compressive nonlinearity predicts no phase shift between contrast modulation and nulling modulation. (B) Sluggish nonlinear feedback model predicts a phase lag for the nulling signal. (C) Sensitivity scaling model in which sensitivity is scaled by a short-term average of recent inputs.

china & Peskin, 1988), the visual system stimulated by a contrast-modulated fringe is an array of linear systems, and arbitrary temporal filtering prior to the nonlinear element (or after it) multiplies the local modulations at later stages by the same factor everywhere. The null condition (zero average modulation) is not changed.

We have investigated the dynamic aspects of the early visual nonlinearity responsible for contrast-modulation flicker by measuring the amplitude and phase of contrast-modulation flicker at different modulation frequencies. Several possible models exist as candidates for the nonlinear mechanism that underlies the observed contrast-modulation flicker. Different models give different predictions for the amplitude and phase dependence on temporal frequency. The simplest scenario (Model A) is an instantaneous nonlinearity: incremental and decremental light sensitivity is scaled instantaneously according to the input intensity, for instance through static response compression in the way depicted in Fig. 6(A). This class of models predicts no phase shift between the nulling signal and the contrast modulation (Appendix).

At the moment of highest contrast, space-averaged output is reduced most, and it is precisely at that moment that the nulling luminance compensation must reach its peak. Another plausible scenario (Model B) is that time-average light exposure reduces sensitivity by shortening integration time, thereby speeding the visual response as well as reducing its sensitivity [Fig. 6(B)]. As will be shown below, this model actually predicts a lag, instead of a lead, for the required nulling signal. Finally (Model C), the units that are responsible for contrast-modulation flicker could set their sensitivity at time  $t$  according to the average input intensity received during a short interval  $\tau$  prior to time  $t - \Delta t$  [Fig. 6(C)]. The results from this experiment can help us to determine which model is most likely and constrain its parameters.

*Procedure*

In the preliminary experiment, as that in Experiment 1, subjects were allowed to vary both amplitude and relative phase of a physical luminance modulation to minimize the perceived contrast-modulation flicker. Two measurements were then made:

1. Based on a preliminary estimate of the nulling amplitude and phase, an individually fixed nulling amplitude [ $A_n$  in equation (2)] was used to find the best nulling phase. A sinusoidal luminance modulation was multiplicatively applied to the contrast-modulated grating [see equation (1) and equation (2) above]. Both the luminance and contrast were modulated at the same frequency, but the relative phase [ $\psi$  in equation (2)] between the contrast modulation and the luminance modulation was under the subject's control. The subject's task was to find the phase where the perceived flicker was minimized. This was then repeated at different modulation frequencies. A precisely appropriate nulling amplitude was not in principle necessary, since the null phase should remain the same with slightly different nulling amplitude.
2. Using the "pedestal-aided nulling" procedure of Experiment 1, nulling amplitude was also carefully measured at different temporal frequencies with relative phase set according to the previous estimate. 30 cycles/deg was the spatial frequency used. Since the flicker signal generated at this spatial frequency was strong, and this spatial frequency is high enough that the modulation of individual bars was not easily detectable, the flicker null was easy to make.

*Results and discussion*

For an optimal null at frequencies in the range 5–25 Hz, the nulling luminance modulation was roughly in phase with the modulation of stimulus contrast, as expected for a compressive or sensitivity-regulating nonlinearity, but the phase match was not exact: the luminance modulation had to anticipate slightly the modulation of contrast, with a phase advance that decreases gradually as a function of temporal frequency

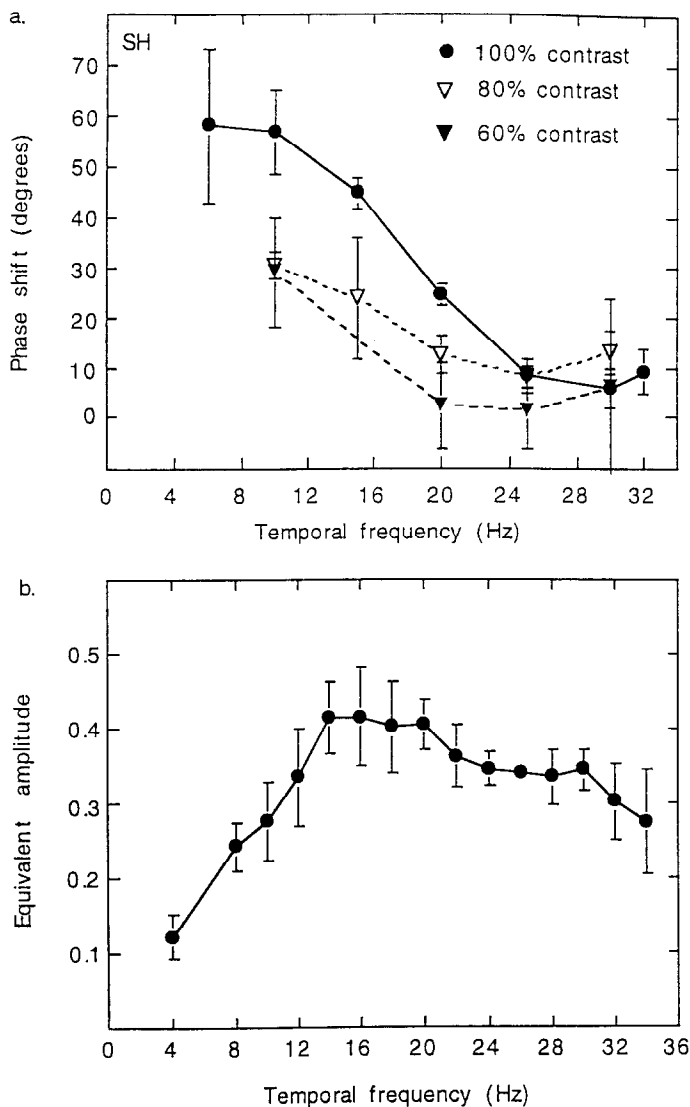


FIGURE 7. (A) Phase of luminance modulation optimally effective in perceptually canceling contrast-modulation flicker for a range of temporal frequencies, spatial frequency at 30 cpd. Positive phase values mean the luminance peak had to precede the contrast peak. Filled circles, 100% peak contrast; open triangles, 80% peak contrast; filled triangles, 60% peak contrast. (B) Amplitude of luminance modulation required to cancel contrast-modulation flicker at different modulation frequencies.

[Fig. 7(A)]\*. The phase advance also depended on the peak contrast of the contrast modulation: the higher the peak contrast, the larger the phase advance.

Figure 7(B) shows how the contrast-modulation flicker amplitude changes with temporal frequency. It has very little attenuation with increasing frequency in the range from 15 Hz to even 30 Hz, which suggests that the underlying mechanism must be very fast, much faster than the visual system as a whole. This idea can be made

\*The identification of the nonlinearity as a compressive one is supported by (1) the polarity of difference-frequency grating (MacLeod *et al.*, 1992), and the polarity of grating contrast required to null them (He & MacLeod, unpublished); and (2) the polarity of contrast-defined grating's input in motion perception (Brown, 1995).

more precise. A key consideration is that the nulling luminance modulation and the contrast modulation, having the same temporal frequency, will undergo similar attenuation due to temporal filtering in linear stages of the system [if spatiotemporal interactions can be neglected, an assumption questioned by Chen and Makous (personal communication)]. Consider the visual system as a sandwich in which linear input and output stages are arranged on either side of the nonlinear element. For our stimulus, the effects of the earlier and later temporal filtering will cancel, leaving these with no influence on the nulling amplitude (see Appendix). Only the nonlinear element itself can introduce a frequency dependence of the nulling amplitude. This makes the nulling method particularly useful as a tool to isolate the nonlinear process for separate characterization. Curiously enough, either the instantaneous nonlinearity (Model A) or at the other extreme a very sluggish sensitivity-scaling mechanism, with an integration time long relative to the stimulus cycle (Model B) predict a nulling amplitude entirely independent of temporal frequency, and are therefore very roughly, but not exactly, consistent with the data. Model C is considered below.

The phase lead required for the nulling signal clearly excludes both Model A and Model B as an idealization of the nonlinear process. The instantaneous nonlinearity (Model A) predicts no phase mismatch [Fig. 6(A)]. Model B, in which time-average light exposure speeds the visual response as well as reducing its sensitivity [Fig. 6(B)], for instance by regulating the gain of a slow inhibitory component in the response to light (Kelly, 1971; Tranchina & Peskin, 1988) predicts a nulling signal lag, not a lead.

Figure 8 illustrates this. It is assumed that the inhibitory signal is a time-average over a period long relative to the stimulus cycle [through filter  $G(f)$  in Fig. 6(B)]. The system then behaves like a different linear one for each different time-average intensity (or for each position in the fringe-illuminated field). The response of the nonlinear element under the bright bar (where average intensity is higher and inhibition stronger) will tend to become biphasic [Fig. 8(A)]. The bright bar frequency response correspondingly becomes bandpass, with a relative advance in phase: the response to the bright bars is reduced in amplitude and has a shorter time to peak compared with response to dim bars.

Figure 8(B) shows the vector analysis of the model. Each local sine wave response is represented as a vector, with phase lead relative to the bright bar response indicated by clockwise rotation from horizontal. For a strictly linear system, regions under a bright bar and regions under a dim bar would give the same response amplitude but with opposite sign, since they both have the same absolute intensity modulation but in opposite phase. But in the sluggish nonlinear feedback model, the array of linear systems responds with different gain and phase depending on their time-averaged light exposure. The reduced gain under the bright bars makes the vector labeled "bright bar response" shorter, and because of the

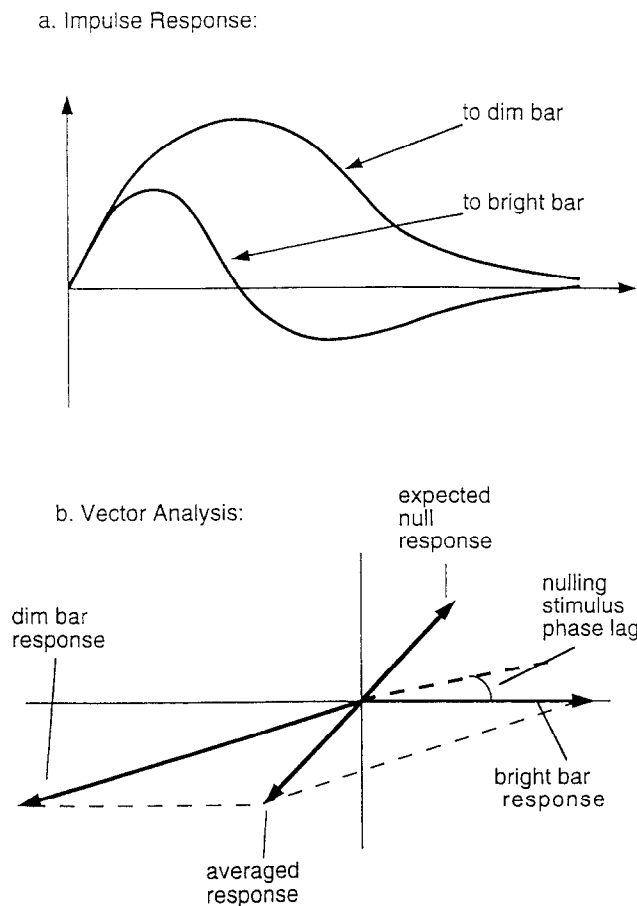


FIGURE 8. Predictions from the sluggish nonlinear feedback model. (A) Impulse response for this model. Receptors under bright bars have higher adaptation levels, which reduce the response peak and speed up the time to reach the peak level compared with receptors under dim bars. (B) Vector analysis. Responses from bright and dim bar regions are different in amplitude and phase, requiring a nulling signal that is phase lagged.

relative phase advance of the bright bar response, the dim bar response vector is rotated anticlockwise from collinearity with the bright bar response vector.

As the dashed parallelogram in Fig. 8(B) illustrates, the resultant space-average signal is dominated by the dim bar response, and has the same or greater lag. The nulling luminance modulation should have to be retarded relative to the bright bar stimulus, in order to produce a response with a similar lag. Data for frequencies to 25 Hz contradict this.

To explain the nulling results, the fundamental component of the dim bar response must have a phase lag less than that for the bright bar, in apparent contradiction to the principle that light adaptation makes visual responses faster. Some models of adaptation do allow this. One example is a sensitivity regulator [Model C, Fig. 6(C)] that simply scales sensitivity roughly in inverse proportion to recent input levels [Fig. 6(C)]. This model (sometimes known as the "dark glasses" model: MacLeod, 1978) differs from Model B in that the sensitivity regulator may take a time-average of the input over an interval short enough to allow the sensitivity to vary substantially during the flicker cycle.

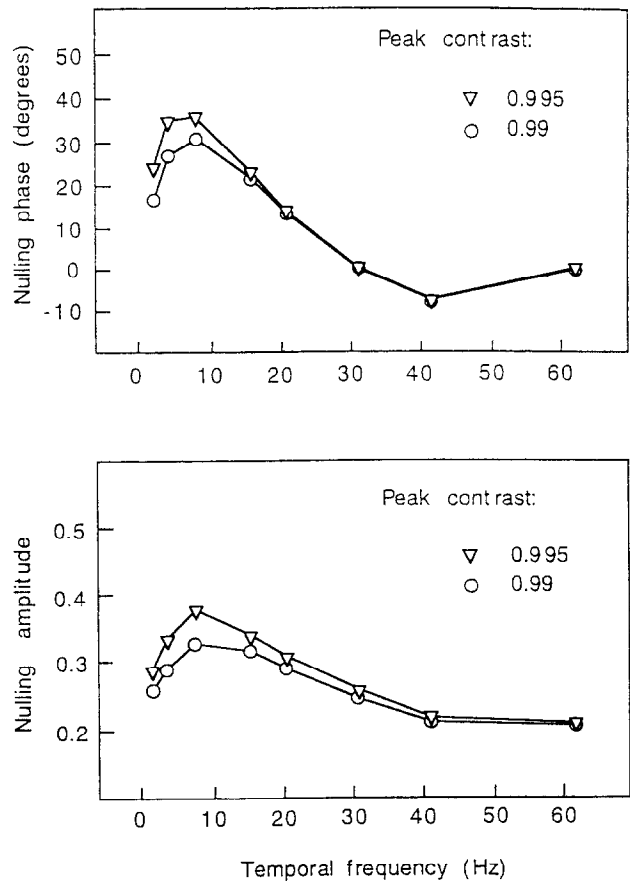


FIGURE 9. Computer simulation results for nulling amplitude and phase using the fast sensitivity scaling model. Parameter values: stimulus contrast 0.995 (triangle) or 0.99 (circle), delay 16 msec, number of RC stages 32. [The corresponding integration time (measured either as impulse response area/height, or full width at half height) for sensitivity control is about 7 msec.]

If the flicker is not too fast for the sensitivity regulator to track, and if the peak contrast of the fringe pattern is high, then sensitivity in the "dim bar" region will briefly be very high shortly after the fringe pattern reaches peak contrast (when the dim bars become dark), and correspondingly large responses will be generated when light begins to return to that region. The space-average response is dominated by the resulting sawtooth-like response in the dim bars, the fundamental component of which is considerably phase-advanced by the sensitivity-regulating mechanism.

Simulations of this simple sensitivity regulator scheme do not fit our data exactly, but they do yield roughly appropriate amplitudes and phases for the null settings in contrast modulation flicker (Fig. 9), and the predicted sawtooth distortion can be seen at low temporal frequencies. A phase approaching zero is predicted when the delay of the sensitivity-regulating signal is equal to half of a flicker cycle, since in this situation, the sensitivity peak coincides with the stimulus peak so that the response will peak at the same time. This can provide an estimate of the effective delay of the sensitivity-regulating signal: it is observed at approx. 25–30 Hz [Fig. 7(A)], so the sensitivity-regulating process must be fast, with an effective delay to peak effect of only 16–20 msec.

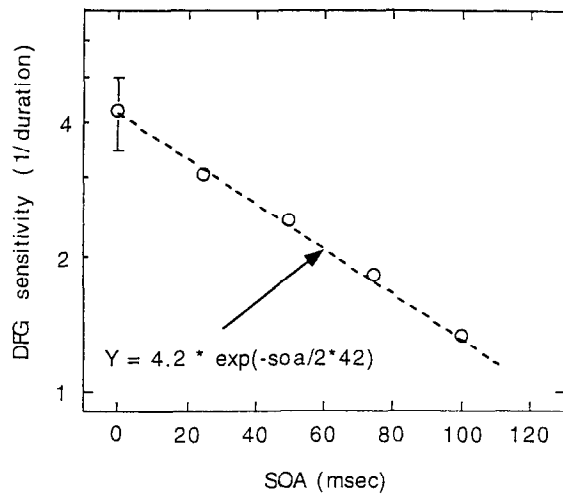


FIGURE 10. Contrast sensitivity for seeing difference-frequency gratings with different SOAs. The exponential function fit to these data corresponds to an integration time of 42 msec for stages up to the nonlinear one.

An independent parameter of the model is the persistence of the sensitivity-regulating signal (the period over which the sensitivity regulator averages previous input to set sensitivity); this is likely on general grounds to be of the same order as the delay, but it has to be somewhat shorter in order for the simulations of this model to recreate the slow decline in equivalent amplitude we observe in the 14–30 Hz range [see Fig. 7(B)]. When the frequency is doubled from 14 to 28 Hz, the contrast-modulation flicker amplitude only goes down from 40% to about 30%. Simulations indicate that in order to duplicate this slow decrease in the nulling amplitude with temporal frequency, the scaling signal must integrate over only about 7 msec (impulse response full-width at half height). In the simulations, the temporal integration of the sensitivity-regulating signal was modeled by a cascade of RC signals of equal time constant. Persistence and effective delay of the sensitivity-regulating signal were varied by varying both the number of the RC stages and their common time constant: for a fixed delay the persistence decreases as the number of stages increases. The curves of Fig. 9 were obtained with 32 stages and a delay of 16 msec. A further parameter of the model was the peak contrast of the input intensity profile, which had to be between 0.99 and 0.995, a reasonable value for an interference fringe pattern. Not only can multiple scatter within the eye degrade the contrast slightly from its theoretical value of unity, but deviations from fully reciprocal sensitivity regulation (such as result from the inclusion of an absolute threshold constant in Weber's Law) are also accommodated by reduction of this model parameter. The values obtained for it suggest that local sensitivity varied more than 100-fold across the fringe pattern.

### Experiment 3: reinstating prior filtering with difference-frequency gratings

We have noted that nulling measurements of contrast-

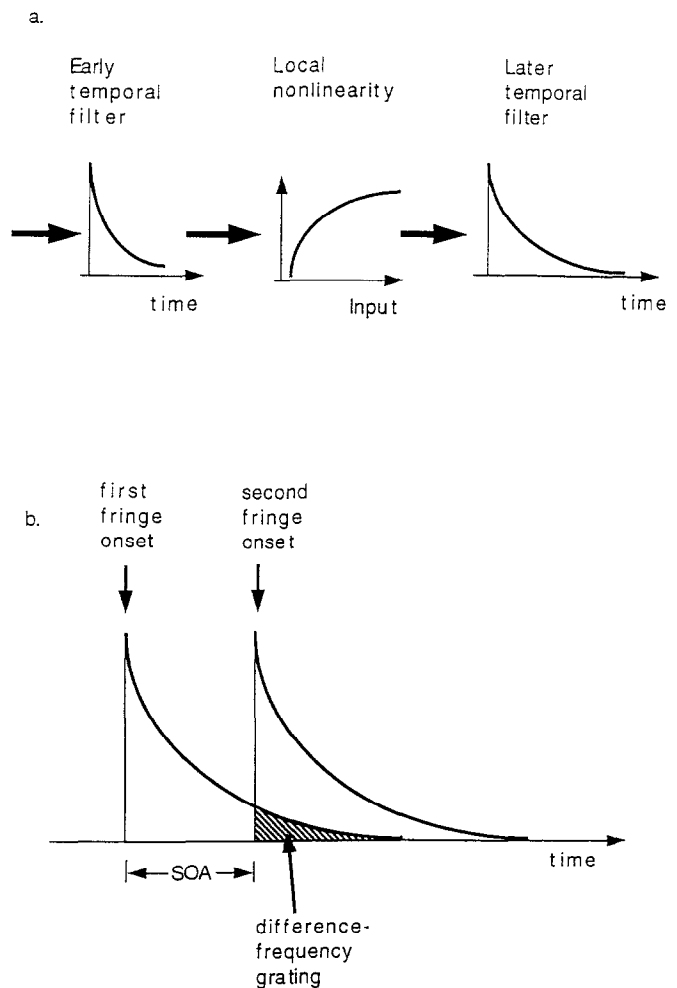


FIGURE 11. How temporal integration prior to the nonlinear element affects difference-frequency grating visibility as a function of the SOAs between the two brief pulses.

modulation flicker may characterize the dynamics of the nonlinear process with little influence of prior or later temporal filtering by the visual system. Usefully, other experimental measures of persistence at the nonlinear stage depend on the effects of prior temporal filtering, as well as on the inherent dynamics of the adapting element, and the comparison of the results can help to characterize the prior filter.

One such experiment is to measure the visibility of difference-frequency gratings (Burton, 1973; MacLeod *et al.*, 1992; Chen *et al.*, 1993) as a function of the time interval when two fringes of slightly different orientation are successively and very briefly interpolated into a uniform field of constant overall luminance (Fig. 10). The experiment is similar to one reported by MacLeod *et al.* (1992). But in that case, the first pulse was of bleaching intensity and delays of seconds could be tolerated. In this case we evaluated persistence at sub-bleaching light levels. For each of a range of onset-time asynchronies (SOA), the duration of the two brief pulses was varied in a forced-choice staircase procedure, and the subject's task was to report whether the difference-frequency grating was vertical or horizontal. The duration that gives

84% correct response in a maximum likelihood fit to the data was then taken as the threshold duration, and sensitivity (vertical axis in Fig. 10) was defined as the reciprocal of this duration. The results can be considered within a theoretical framework in which an early linear temporal filter precedes the nonlinear element, and this is in turn followed by a later linear filter [Fig. 11(A)]. The perception of the difference-frequency grating depends on the product of the fringe effective contrasts at the nonlinear stage, as viewed through the later filter. Assuming (because it turns out to agree with the data) a simple exponential decay for the early temporal filter,  $\exp(-t/\tau)$ , then the difference-frequency grating depends on the shaded area in Fig. 11(B). The first fringe pattern is attenuated by  $\exp(-SOA/\tau)$  at the nonlinear site at the time the second pulse was delivered; assuming complete temporal integration for the pulse duration, the time course of the two-pulse product is:

$$d^2 \exp(-(2t - SOA)/\tau)$$

where  $d$  is the pulse duration and  $t$  is the time since onset of the first pulse. Any weighted time-integral of this expression [such as might be derived by the later temporal filter of Fig. 11(A)] will retain the exponential dependence on SOA. Consequently, if thresholds for the different SOAs are determined by any such integral (i.e., by any subsequent filtering of the output from the nonlinear stage), the above expression must be constant at threshold, so threshold sensitivity is given by

$$1/d = C \exp(-SOA/2\tau)$$

independent of the characteristics of the later filter which affect only the constant  $C$ . In Fig. 10 the data of SH are well fit by the equation above with  $\tau = 42$  msec. Data for DM are fit by  $\tau = 30$  msec. The results indicate substantial persistence prior to the nonlinear stage (as might be expected from the validity of the Talbot-Plateau Law): an exponential time constant of 30 or 40 msec, or perhaps a little less given that the sensitivity regulator itself introduces some temporal integration in the generation of its distortion products.

*Experiment 4: dependence of contrast-modulation flicker on mean luminance*

Contrast-modulation flicker is visible down to low photopic light levels. Figure 12 shows the contrast-modulation flicker nulling amplitude as a function of average luminance level, for a stimulus of unity peak contrast. In Fig. 12 the experimental amplitudes are fitted by a curve based on the simple idea that the effective contrast of the interference fringe pattern is degraded at low intensities as if by the addition of a uniform intensity  $I_0$ , thus contrast =  $I/(I + I_0)$ . The value of  $I_0$  required for the fit is 44 trolands. This is the background that is just sufficient to halve the sensitivity of the local adaptation process. It is as low as the lowest comparable values for visual contrast thresholds at high spatial frequencies (Van Nes & Bouman, 1967), indicating that the local adaptation responsible for contrast-modulation flicker accounts for all or almost all of the visual system's

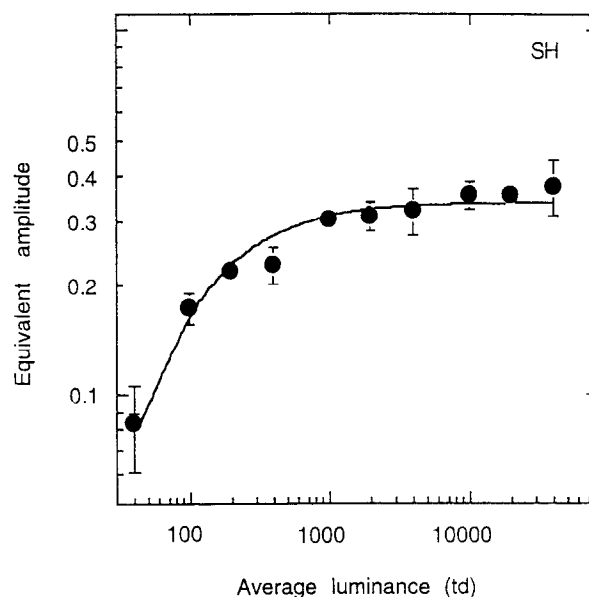


FIGURE 12. Contrast-modulation flicker measured for different space-average luminance levels. The curve was obtained assuming a reduction of effective contrast with decreasing luminance in accordance with the equation  $C = k * I / (I + I_0)$ , with  $I_0 = 44$  trolands,  $k$  is a constant.

regulation of its sensitivity to these patterns. Burton (1973) and Makous, MacLeod and Williams (1985) found similar values for another product of local non-linearity, the difference-frequency grating. This lower limit of intensity for contrast-modulation flicker is comparable with the lower limit for adaptation in monkey gross receptor potentials (Boynton & Whitten, 1970), but is far below the range for adaptation in the cone outer segment photocurrent (Schnapf, Nunn, Meister & Baylor, 1990).

**GENERAL DISCUSSION**

*Local nature of the underlying mechanism: anatomical and psychophysical comparisons*

Our observations support the idea that contrast-modulation flicker arises from a strictly local and very

TABLE 1. Table 1. Psychophysics (including data from MacLeod *et al.*, 1992; Chen *et al.*, 1993)

Technique	Observer	Full width at half height (arc sec)
DFG	WM (1992)	16.6
DFG	DW (1992)	12.6
DFG	DM (1992)	11.9
DFG	BC (1993)	21.5
CMF	RS (present)	19.0
CMF	SH (present)	17.2
CMF	DM (present)	14.5
Anatomy (data from Curcio, 1987)		
Inner segment diameter		28

fast sensitivity regulating mechanism in the visual response to light. Just how local is illustrated in Fig. 4(B) with an estimated point spread function at the nonlinear site, compared with a schematic diagram of a foveal cone. The estimate from contrast-modulation flicker technique is very similar to that derived from threshold measurements of another nonlinear distortion product, difference-frequency gratings (Chen *et al.*, 1993; MacLeod *et al.*, 1992). Table 1 lists the estimated width at half height of the gaussian point spread function at the input to the nonlinear site from both psychophysical techniques. Anatomical estimates of foveal cone size (Curcio, 1987) are also included for comparison.

In general, this point spread function is slightly smaller than the cone inner segment diameter, with an average full width at half height of 16.2 arc sec. This leaves no margin for any neural spatial integration: the nonlinear process must be strictly local, either inside the cones or else fed by pure signals from individual receptors without any significant contribution from nearby cones. This conclusion needs to be qualified. The data of Fig. 4(A) extend down only to 32 cpd, so the gaussian that we fit to them may not apply at lower frequencies. The input to the nonlinear element may correspondingly include a diffuse component, as well as a strictly local one. Indeed, Chen *et al.* (1993) in their study of difference-frequency gratings did find evidence for a reduced transmission of low spatial frequencies to the nonlinear site, suggesting a spatial antagonism preceding the local nonlinearity. On the other hand, Pelli (1986) (and in preparation) infers from experiments on the perceived mark/space ratio in complex gratings that what is probably the same nonlinearity appears still to be strictly local, even when assessed across the low-frequency range. But in any case, the amplitude of contrast-modulation flicker at high spatial frequencies is enough to imply that the strictly local and rapid variation in sensitivity across a fringe pattern is substantial. In our simulations, appropriate amplitudes required a nearly reciprocal (Weber Law) sensitivity adjustment and a near-unity peak contrast at the adapting site—a situation in which the model's rapidly set local sensitivity varies by a factor of more than 50 across the fringe pattern.

Observer DM has data from both difference-frequency grating method and the contrast-modulation flicker measurements. Estimates of point spread function from the two methods on this same observer are in good agreement, although the contrast-modulation flicker method gives a slightly higher estimate (full width at half height: 14.5 vs 11.9 arc sec). In general, the widths of the cone apertures estimated from contrast-modulation flicker tend to be a little larger than those from difference-frequency grating experiments. This may not be a fundamental inconsistency. Flicker detection undoubtedly depends more on the relatively poorly resolving retina near the margin of the stimulus field than does pattern resolution, and cone size is strongly eccentricity dependent, increasing by a factor of 1.4 from the central

fovea to an eccentricity of 30' (based on Fig. 6 of Curcio, Sloan, Kalina & Hendrickson, 1990). Thus, the cone photoreceptors critical for flicker detection are larger than those that subserve pattern resolution.

The spatial frequency response at the nonlinear element might in principle be spuriously extended by aliasing with the cone mosaic. This raises the question whether a model with aliasing, followed by spatial integration, followed by adaptation could account for our observations without any strictly local nonlinearity. But as argued elsewhere (He & MacLeod, 1996; MacLeod *et al.*, 1992), such a model incorrectly predicts a dip in distortion product amplitude around the Nyquist frequency. No such dip is seen in Fig. 4. Indeed, we have shown (He & MacLeod, 1996) that it is spatially uniform cues due to local nonlinearity, and not aliasing that generally support the detection of gratings in that frequency range.

It is of considerable interest that the nonlinearity underlying contrast-modulation flicker is just as local as the one underlying difference-frequency gratings. Flicker detection is presumably mediated by different postreceptoral cells, with larger receptive fields, than those that represent spatial details such as a difference-frequency grating (King-Smith & Kulikowski, 1975; Kulikowski & Tolhurst, 1973; Lee, Martin & Valberg, 1988; Livingstone & Hubel, 1987). If this difference in receptive field size were already present at the input to the nonlinear elements, then difference-frequency gratings and contrast-modulation flicker might originate respectively from a local nonlinearity (at, for instance, midget bipolar cells), and one that is preceded by some spatial integration (perhaps at diffuse bipolars). Our results are inconsistent with any such scenario and thus encourage the conclusion that the nonlinearity is linked to the cones themselves. There is some evidence that the cone inputs to different neural pathways (chromatic and monochromatic) can be selectively suppressed by different factors for the different pathways (Ahn & MacLeod, 1993). The synapses between the cones and different bipolars are a possible site for pathway-specific adaptation that might be strictly local in the sense required by our results. Synaptic nonlinearity is pervasive in the nervous system and an effectively compressive synaptic nonlinearity has been demonstrated in toad rods (Belgum & Copenhagen, 1988). A synaptic locus for local nonlinearity would reconcile the psychophysical data with the cone out-segment photocurrent recordings (Schnapf *et al.*, 1990) that show linear behavior at the intensity levels of our experiments.

Rushton (1965) famously argued that in human rod vision, strictly local processes make no contribution at all to light adaptation. This would be utterly at variance with the present findings but for the fact that the present results refer not to rod, but to cone vision. As Rushton's view requires, contrast-modulation flicker, like difference-frequency gratings, is conspicuous by its absence in rod vision (MacLeod, Chen & Crognale, 1989; MacLeod & He, 1993; MacLeod *et al.*, 1992). It should not be

surprising that the rod and cone systems differ so completely in this regard: owing to the very low quantum fluxes present in scotopic conditions, individual rods have no opportunity to make a rapid assessment of the prevailing light level, and so the job of regulating sensitivity must be undertaken by collectives of rods, perhaps through neural convergence prior to the adaptation mechanism. Thus, in both rod and cone systems, the regulation of sensitivity is handled early, but not—as would occur if individual rods regulated their sensitivity—too early. The adaptation mechanisms in rod and cone outer segments (e.g. Schnapf *et al.*, 1990; Koutalos & Yau, 1996) have no substantial influence on adaptation over most of the intensity range, since they come into play only at very high intensities.

#### *Intensity dependence*

The suggestion that cones have their own sensitivity control is noteworthy, because the light levels in these experiments are far less than the levels required to achieve substantial regulation of sensitivity for the cone outer segment photocurrent (Schnapf *et al.*, 1990). On the other hand, the intensity range for adaptation in the gross receptor potential in monkeys does extend low enough to include our stimulus level (Boynton & Whitten, 1970; Valeton & van Norren, 1983; Hood & Birch, 1993). In our experiment (Fig. 12), contrast-modulation flicker is demonstrable in cone vision over an intensity range similar to that found for receptor potentials. Both receptor potentials and psychophysics could be affected by inner segment adaptation processes such as voltage-sensitive conductances.

Contrast-modulation flicker is little affected by changes in intensity down to quite low light levels (Fig. 12), much like psychophysical contrast thresholds. Evidently most or all of the sensitivity regulation implicit in Weber's Law has already been implemented when the visual signal emerges from the nonlinear stage. This makes it tempting to assume that virtually all light adaptation in the cone system is strictly local. But many observations using conventional stimuli indicate otherwise: for instance the results of Cicerone, Hayhoe and MacLeod (1990) indicate that adaptation in the cone system involves very little spreading, but probably more than can be explained by purely optical causes. This is also implied by the numerous investigations (e.g. Stiles, 1959) that show deviations from independence of the different cone types in sensitivity regulation.

#### *Rapid dynamics*

Although there is still a tendency to think of adaptation as a slow process, both psychophysics and neurophysiology have shown major adjustments of sensitivity that proceed very rapidly. Notably, work on the photoreceptors reveals powerful sensitivity-regulating mechanisms that operate on a time scale of milliseconds (e.g. Baylor & Hodgkin, 1974; Lamb, 1985; Lamb & Pugh, 1992). The receptor outer segment rapid adaptation processes currently being intensively investigated may

not, however, be relevant for human vision, since primate receptor outer segments appear to lack sensitivity control in the relevant intensity range (Schnapf *et al.*, 1990; Walraven *et al.*, 1990). There is also psychophysical evidence for rapid adaptation. Indeed, threshold measurements on time-modulated backgrounds (Boynton, Sturr & Ikeda, 1961; Bone, McTavish & Tang, 1991; Crawford, 1947; Hayhoe, Benimoff & Hood, 1987; Powers & Robson, 1987; Robson, 1966) in some cases suggest an even faster kinetics for adaptive sensitivity changes than proposed here. Our experiments are unique, however, in that a null is set at the output of the nonlinear element, hence before spatial integration. This should help isolate the primary adaptation mechanism for dynamic characterization, because masking effects by transient "on-effects" at later stages of the system are likely to be bypassed.

#### *Some problematic observations*

*Low frequency phase reversal.* The fast sensitivity-regulation model seems to be roughly consistent with most of our contrast-modulation flicker data, but there is one exception. A sustained fringe actually appears *brighter* than a uniform field of the same space-average luminance (Campbell & Green, 1965; He & MacLeod, 1996). Correspondingly, in the present experiments, we have noted that for slow (below 4 Hz) modulation of fringe contrast, the nulling luminance modulation is inverted in phase, relative to what we have reported for rapid modulation. We have not stressed this, in part because the nulls at low temporal frequencies are very poorly defined, but it presents a problem for the fast scaler model: if temporal integration by the filter embedded in the sensitivity regulator element in Fig. 6 is monotonic, the model predicts a decrease, but not a reversal, in the phase offset of the nulling signal [see Fig. 9(A)]. Nor does it predict a possibly related observation, the observed loss of contrast-modulation flicker amplitude at low temporal frequencies (Fig. 7). To explain these phenomena, one might appeal to the fact that at a stage following the compressive nonlinearity, contrast-sensitive neurons have a rectification-like (positively accelerated) threshold nonlinearity in their response to local contrast. A fringe pattern will be a better stimulus to such neurons than a uniform field, even if there is a compressive transformation of luminance at their inputs. The question then arises why this putative rectifying nonlinearity does not influence the nulls at high temporal frequencies, which we here interpret in terms of a compressive nonlinearity (more accurately, a fast sensitivity scaling mechanism) alone. One answer is as follows. There is evidence that the smallest cells do not support the perception of rapid flicker, and that perception of rapid flicker depends instead on changes in a linearly integrated space-average of cone signals over a neighborhood large relative to our fringe pattern period (Kelly, 1971; King-Smith & Kulikowski, 1975; Kulikowski & Tolhurst, 1973; Robson, 1966). Whatever new nonlinear transformations the resulting flicker signal

undergoes, the null condition will be the one that holds that space-average cone output constant. This will reflect only the early, local nonlinearity characterized here. For perception of lower-frequency fluctuations, early spatial integration may be more restricted or absent, allowing the more central nonlinearities to influence the response to contrast-modulated stimuli in those cases.

*High-frequency linearity.* The model as shown in Fig. 11 cannot account for "high-frequency linearity"—the observation that while light adaptation reduces sensitivity at low frequencies, it fully preserves sensitivity for sufficiently fast flicker. Under our conditions, however, we have measured the loss of sensitivity with change in mean luminance from 500 td (dim bar time-average) to 1500 td (bright bar time-average) and find it to be almost independent of frequency in the 5–35 Hz range we deal with: Weber's Law roughly holds across this range. To give an account of flicker sensitivity at still higher frequencies, or lower luminances, where an approach to high-frequency linearity is evident, requires a more elaborate conception of the effects of adaptation—for instance inhibitory gain-regulation schemes as proposed by Kelly and Tranchina, or parametric control schemes in which it is the time constants of transduction stages, rather than simply sensitivity, that are adaptively adjusted. The simple "dark glasses" scaler may work for our present data because it is an asymptotically realized simplification of these other schemes. But whatever the precise effects of adaptation may be, they must be imposed very rapidly, as in some proposals (Baylor *et al.*, 1974; Sperling & Sondhi, 1968; Graham & Hood, 1992) they are, to account for our results.

*Dynamics of sensation: preservation of low temporal frequencies.* With a very fast, local and reciprocal adjustment of sensitivity, the output of each cone's sensitivity scaler will become independent of the input intensity in a rapidly approached steady state, and one might expect that things should disappear rapidly if the image remains static. Yet though stabilized images do fade, they remain visible for several seconds before fading becomes complete. Slow fading could be consistent with fast local sensitivity adjustments if (1) the adjustment is not quite fully reciprocal, so the steady-state output of the nonlinear element does show some dependence on input intensity, and this supports vision until a more central processing element with a poor response to steady input filters it out; or (2) the temporal transients created by eye movements may be rectified and integrated over a period that can (at least for a steady, stabilized image) be long by comparison with the time constants of the adaptation process. A related problem is that a fast adaptation process should make slow (e.g. 2 Hz) flicker much less visible than faster (say, 10 Hz) flicker, yet this is not always observed (Kelly, 1971; Robson, 1966). Perhaps low-pass filtering preceding or following the adapting element roughly cancels or outweighs the adaptation effect in these cases.

## CONCLUSIONS

Contrast-modulation flicker effect originates from a strictly local nonlinearity in the visual response to light—to generate it, the fringe has to be resolved at the photoreceptors, but can be much too fine to be resolved perceptually. Contrast-modulation flicker shares this and other characteristics, including intensity range, with difference-frequency gratings. The responsible nonlinearity is a fast (roughly 20 msec delay) sensitivity-regulating mechanism, specific to individual photoreceptors, and operative in human cone, but not rod vision.

## REFERENCES

- Ahn, S. J. & MacLeod, D. I. A. (1993). Link-specific adaptation in the chromatic and luminance channels. *Vision Research*, *33*, 2271–2286.
- Baylor, D. A., Fuortes, M. G. F. & O'Bryan, P. M. (1971). Receptive fields of single cones in the retina of the turtle. *Journal of Physiology (London)*, *214*, 265–294.
- Baylor, D. A. & Hodgkin, A. L. (1974). Changes in time scale and sensitivity in turtle photoreceptors. *Journal of Physiology (London)*, *242*, 729–758.
- Baylor, D. A., Hodgkin, A. L. & Lamb, T. D. (1974). The electrical response of turtle cones to flashes and steps of light. *Journal of Physiology (London)*, *242*, 685–727.
- Belgum, J. & Copenhagen, D. R. (1988). Synaptic transfer of rod signals to horizontal and bipolar cells in the retina of the toad (*Bufo marinus*). *Journal of Physiology*, *396*, 667–680.
- Bone, R. A., McTavish, J. & Tang, J. P. (1991). Gain and phase characteristics of temporal processing determined by increment thresholds. *Investigative Ophthalmology & Visual Science, Supplement*, *32*, 840.
- Boynton, R. M. & Whitten, D. N. (1970). Visual adaptation in monkey cones: recordings of late receptor potentials. *Science*, *170*, 1423–1426.
- Boynton, R. M., Sturr, J. F. & Ikeda, M. (1961). Study of flicker by increment threshold technique. *Journal of the Optical Society of America*, *51*, 196–201.
- Brown, R. O. (1995). Luminance nonlinearities and second-order stimuli. *Investigative Ophthalmology & Visual Science, Supplement*, *36*, 242.
- Burton, G. J. (1973). Evidence for non-linear response processes in the human visual system from measurements on the thresholds of spatial beat frequencies. *Vision Research*, *13*, 1211–1225.
- Campbell, F. W. & Green, D. G. (1965). Optical and retinal factors affecting visual resolution. *Journal of Physiology, London*, *414*, 89–109.
- Chaparro, A., Stromeyer, C. F., Chen, G. & Kronauer, R. E. (1995). Human cones appear to adapt at low light levels: measurements on the red-green detection mechanism. *Vision Research*, *35*, 3103–3118.
- Chen, B., Makous, W. & Williams, D. R. (1993). Serial spatial filters in vision. *Vision Research*, *33*, 413–427.
- Cicerone, C. M., Hayhoe, M. M. & MacLeod, D. I. (1990). The spread of adaptation in human foveal and parafoveal cone vision. *Vision Research*, *30*, 1603–1615.
- Crawford, B. H. (1947). Visual adaptation in relation to brief conditioning stimuli. *Proceedings of the Royal Society of London B*, *134*, 283–302.
- Curcio, C. A. (1987). Diameters of presumed cone apertures in the human retina. *Journal of the Optical Society of America A*, *4*, 70.
- Curcio, C. A., Sloan, K. R., Kalina, R. E. & Hendrickson, A. E. (1990). Human photoreceptor topography. *Journal of Comparative Neurology*, *292*, 497–523.

- Dewar, J. & MacKendrick, J. G. (1873). On the physiological action of the light. *Transactions of the Royal Society of Edinburgh*, 27, 141.
- Fechner, G. T. (1860). *Elemente der Psychophysik*. Leipzig: Breitkopf and Hertel.
- Graham, N. & Hood, D. C. (1992). Modeling the dynamics of light adaptation: the merging of two traditions. *Vision Research*, 32, 1373–1393.
- Green, D. G. (1986). The search for the site of visual adaptation. *Vision Research*, 26, 1417–1430.
- Hayhoe, M., Benimoff, N. I. & Hood, D. C. (1987). The time-course of multiplicative and subtractive adaptation processes. *Vision Research*, 27, 1981–1996.
- He, S. & MacLeod, D. I. A. (1996). Local luminance nonlinearity and receptor aliasing in the detection of high frequency gratings. *Journal of the Optical Society of America A*, 13, 1139–1151.
- Hood, D. C. & Birch, D. G. (1993). Human cone receptor activity: the leading edge of the  $a$ -wave and models of receptor activity. *Visual Neuroscience*, 10, 857–871.
- Kelly, D. H. (1961). Visual responses to time-dependent stimuli I. Amplitude sensitivity measurements. *Journal of the Optical Society of America*, 51, 422–429.
- Kelly, D. H. (1971). Theory of flicker and transient responses, II. Counterphase gratings. *Journal of the Optical Society of America*, 61, 632–640.
- King-Smith, P. E. & Kulikowski, J. J. (1975). Pattern and flicker detection analyzed by subthreshold summation. *Journal of Physiology (London)*, 249, 519–548.
- Koutalos, Y. & Yau, K.-W. (1996). Regulation of sensitivity in vertebrate rod photoreceptors by calcium. *Trends in Neuroscience*, 19, 73–81.
- Kulikowski, J. J. & Tolhurst, D. J. (1973). Psychophysical evidence for sustained and transient channels in human vision. *Journal of Physiology*, 232, 149–163.
- Lamb, T. D. (1985). Properties of cone photoreceptors in relation to color vision. In D. Ottoson & S. Zeki (Eds), *Central and peripheral mechanisms of color vision*. London: Macmillan.
- Lamb, T. D. & Pugh, E. N. J. (1992). A quantitative account of the activation steps involved in phototransduction in amphibian photoreceptors. *Journal of Physiology (London)*, 449, 719–758.
- Lee, B. B., Martin, P. R. & Valberg, A. (1988). The physiological basis of heterochromatic flicker photometry demonstrated in the ganglion cells of the macaque retina. *Journal of Physiology (London)*, 404, 323–347.
- Livingstone, M. S. & Hubel, D. H. (1987). Psychophysical evidence for separate channels for the perception of form, color, movement, and depth. *Journal of Neuroscience*, 7, 3416–3468.
- MacLeod, D. I. A. (1978). Visual sensitivity. *Annual Review of Psychology*, 29, 613–645.
- MacLeod, D. I. A., Chen, B. & Crognale, M. (1989). Spatial organization of sensitivity regulation in rod vision. *Vision Research*, 28, 965–978.
- MacLeod, D. I. A. & He, S. (1993). Visible flicker from invisible patterns. *Nature*, 361, 256–258.
- MacLeod, D. I. A., Williams, D. R. & Makous, W. (1992). A visual nonlinearity fed by single cones. *Vision Research*, 32, 347–363.
- Makous, W., MacLeod, D. I. A. & Williams, D. R. (1985). Nonlinear transformation in human vision. *Journal of the Optical Society of America A*, 2, 1366.
- Maxwell, J. C. (1860). On the theory of compound colours and the relations of the colours of the spectrum. *Philosophical Transactions of the Royal Society*, 150, 57–84.
- Pelli, D. G. (1986). Bright areas appear magnified: a visual saturation? *Investigative Ophthalmology & Visual Science, Supplement*, 27, 226.
- Polyak, S. L. (1941). *The retina*. Chicago: University of Chicago Press.
- Powers, M. K. & Robson, J. G. (1987). Sensitivity changes induced by temporal modulation of a background. *Investigative Ophthalmology & Visual Science, Supplement*, 28, 357.
- Robson, J. G. (1966). Spatial and temporal contrast sensitivity functions of the visual system. *Journal of the Optical Society of America*, 56, 1141–1142.
- Rushton, W. A. H. (1965). The Ferrier lecture, 1962: Visual adaptation. *Proceedings of the Royal Society of London B*, 16, 20–46.
- Schnapf, J., Nunn Meister, M. & Baylor, D. A. (1990). Visual transduction in cones of the monkey *Macaca fascicularis*. *Journal of Physiology*, 427, 681–713.
- Shapley, R. M. & Enroth-Cugell, C. (1984). Visual adaptation and retinal gain control. *Progress in Retinal Research*, 3, 263–346.
- Sperling, G. & Sondhi, M. M. (1968). Model for visual luminance discrimination and flicker detection. *Journal of the Optical Society of America*, 58, 1133–1145.
- Stiles, W. S. (1959). Color vision: the approach through increment threshold sensitivity. *Proceedings of the National Academy of Sciences USA*, 45, 100–114.
- Tranchina, D. & Peskin, C. S. (1988). Light adaptation in the turtle retina: embedding a parametric family of linear models in a single non-linear model. *Visual Neuroscience*, 1, 339–348.
- Valeton, J. M. & van Norren, D. (1983). Light adaptation of primate cones: an analysis based on extracellular data. *Vision Research*, 23, 1726–1734.
- Van Nes, F. L. & Bouman, M. A. (1967). Spatial modulation transfer in the human eye. *Journal of the Optical Society of America*, 57, 401–406.
- Walraven, J., Enroth-Cugell, C., Hood, D. C., MacLeod, D. I. A. & Schnapf, J. (1990). The control of visual sensitivity: receptor and postreceptor processes. In L. Spillman & J. S. Werner (Eds), *Visual perception: the neurophysiological foundations* (pp. 53–101). New York: Academic Press.
- Williams, D. R. & MacLeod, D. I. A. (1979). Interchangeable backgrounds for cone images. *Vision Research*, 19, 867–878.

*Acknowledgements*—This work was supported by NIH grant EY-01711. We thank Walter Makous for comments on a draft.

## APPENDIX

### *Quantitative estimation of spatial and temporal resolution for the nonlinear mechanism*

We give here an analysis of the response of an instantaneous nonlinearity to contrast modulation, with the help of somewhat unrealistic simplifying assumptions, since even a crude idealization may provide useful intuition. The analysis is only loosely relevant to the sensitivity scaler model, and our tests of that (Fig. 12) rely on computer simulations rather than analysis.

Represent the attenuation of spatial contrast that a stimulus undergoes due to linear spatial integration preceding the nonlinear site by the transmission factor  $S(f_x)$ , and the temporal transmission factor by  $T(f_t)$  with phase lag  $\phi(f_t)$ . Then at the input to the nonlinear site, the stimulus intensity distribution of equation (1) will give rise to a linear input,  $I(x, t)$ :

$$I(x, t) = I_m \{ 1 + CS(f_x) \cos(2\pi f_x x) [(1 + T(f_t) \cos(2\pi f_t t + \phi(f_t)))/2] \}. \quad (A1)$$

It is convenient to consider the deviation of the above signal from its space-average level:

$$\xi(x, t) = I_m CS(f_x) \cos(2\pi f_x x) [1 + T(f_t) \cos(2\pi f_t t + \phi(f_t))]/2. \quad (A2)$$

The contrast-modulation flicker depends on  $\xi(x, t)$  and the form of the nonlinearity that  $\xi(x, t)$  will undergo. For a smooth instantaneous nonlinearity and a small signal the response can be approximated by the linear and quadratic terms in the power series of  $\xi(x, t)$ ,

$$R(x, t) = c_1 \xi(x, t) + c_2 \xi^2(x, t). \quad (A3)$$

To make this account of adaptation in terms of a static nonlinearity reasonably realistic, the coefficients  $c_1$  and  $c_2$  must depend strongly on the mean intensity  $I_m$ , but this dependence on mean intensity is not considered here. We can determine how the space-average output at the nonlinear site fluctuates over time by substituting A(2) into A(3); over each spatial cycle, the term in  $\xi(x, t)$  integrates to zero for all  $t$ ,

creating no contrast-modulation flicker, but the term in  $\xi^2(x,t)$  integrates to:

$$\left( c_2 I_m^2 C^2 S^2(f_x) \int_0^1 \cos^2(2\pi u) du \right) [1 + T(f_i) \cos(2\pi f_i t + \phi(f_i)) / 2]^2, \quad (\text{A4})$$

where  $u = f_x x$ .

Since the integral  $\int_0^1 \cos^2(2\pi u) du$  evaluates to 1/2, after dropping the time-independent term, the above expression becomes

$$\begin{aligned} & (c_2/2) [I_m CS(f_x)]^2 T(f_i) \cos(2\pi f_i t + \phi(f_i)) \\ & + (c_2/8) [I_m CS(f_x) T(f_i)]^2 \cos(4\pi f_i t + 2\phi(f_i)). \end{aligned} \quad (\text{A5})$$

The first and second term above represent the fundamental and the second harmonic of the contrast-modulation flicker, respectively. The fundamental amplitude is proportional to the temporal transmission factor  $T(f_i)$ , to the square of the peak contrast of the grating  $C$ , and to the square of the spatial transmission factor  $S(f_x)$ . If we neglect for simplicity the nonlinear components of the response to the nulling modulation itself (and if we neglect spatiotemporal interaction that could differently affect the temporal response to uniform and patterned stimuli prior to the nonlinear stage), then the amplitude of the response to a spatially uniform nulling modulation  $A_n$  at the output of the nonlinear site is simply  $c_1 I_m A_n T(f_i)$ , being subject to attenuation by

temporal filtering only and not by spatial filtering, and the phase lag at every point is the appropriate one  $\phi(f_i)$ . For this to cancel the contrast-modulation fundamental component from A(5),  $A_n$  must satisfy:

$$c_1 I_m A_n T(f_i) = (c_2/2) [I_m CS(f_x)]^2 T(f_i)$$

or

$$A_n = I_m (c_2/2c_1) [CS(f_x)]^2. \quad (\text{A6})$$

The implied increase of nulling amplitude with the square of the peak contrast (and its independence of temporal frequency) are roughly consistent with our results.

To characterize the system's spatial resolution we measured  $A_n$  as a function of  $f_x$ , then applied A(6) to estimate  $S(f_x)$ . The estimated  $S(f_x)$  was then fitted (least squares) with the gaussian curve:

$$S(f_x) = k \exp(-2\pi^2 f_x^2 \sigma^2). \quad (\text{A7})$$

The Fourier transform of A(7) gives the corresponding symmetrical line point spread function  $g(x)$ , or, to within a height-scaling constant, the point spread function:

$$g(x) = [k / ((2\pi)^{0.5} \sigma)] \exp(-x^2 / 2\sigma^2). \quad (\text{A8})$$

The full width at half height of this point spread function corresponds to  $x = 2.35\sigma$ , which was the number given in Table 1.